The mechanism of remdesivir inhibition of propranolol metabolism using an *in vitro* model

A thesis submitted by

Siyu Li

in partial fulfillment of the requirements for the degree of

Master of Science

in

Pharmacology and Drug Development

Tufts University

Graduate School of Biomedical Sciences

May 2021

Advisor: David J. Greenblatt, M.D.

James D. Baleja, Ph.D.

Abstract

Propranolol is a non-selective beta blocker used as the treatment for hypertension, angina, and cardiac arrhythmia. It has three major metabolic pathways: ring hydroxylation, side-chain oxidation, and glucuronidation. Ring hydroxylation of propranolol is mainly carried out by cytochrome P450 (CYP) 2D6, and side-chain oxidation is dependent on CYP1A2. In addition, propranolol is transformed to propranolol glucuronide through uridine 5'-diphospho-glucuronosyltransferase (UGT) metabolism. Remdesivir (GS-5734) is a nucleoside analogue prodrug that inhibits viral replication by delayed chain termination induced by its interaction with RNA dependent RNA polymerase (RdRp). Remdesivir is also a substrate of CYP2D6, and weakly inhibits CYP2D6 and CYP3A4. In this study, we first identified propranolol and its metabolites using high performance liquid chromatography-ultraviolet detection (HPLC-UV) and HPLC-fluorescence detection (HPLC-FLD). We then evaluated the kinetic models of each metabolite: Km values were 19.8 uM, 18.0 uM and 284 uM for 4-hydroxypropranolol (4-OH PPL), 5-hydroxypropranolol (5-OH PPL) and propranolol glucuronide, respectively, upon incubation with pooled human liver microsomes (HLM). We next investigated the inhibition effect of remdesivir on propranolol metabolism, and obtained the results that high concentrations of remdesivir produced approximately 50% inhibition of propranolol metabolism at 15 uM propranolol.

Acknowledgements

Throughout the writing of this thesis, I have received a great deal of support and assistance.

First and foremost, I would like to express my sincere gratitude to my supervisors, Dr. David. J. Greenblatt and Dr. James Baleja for their insightful suggestions, continuous support, and patience during my thesis work.

I would like to offer my special thanks to my lab mate, Mr. Qingchen Zhang. This thesis work could not be finished without his help and advices. Also, I am very grateful to Ms. Suxiang Duan for her technical support.

I would also like to thank my friends, Zixuan Hao, Qianni Ma, Shiyun Wang and Bohan Chang, who helped me to build confidence and shared happiness and sadness together.

Last but not least, my appreciation also goes out to my family and my boyfriend for their encouragement and support all through my studies.

Table of Contents

List of Tables

List of Figures

List of Abbreviations

4-OH PPL: 4-hydroxypropranolol
5-OH PPL: 5-hydroxypropranolol
CES1: carboxylesterase 1
COVID-19: coronavirus disease 2019
CYP: cytochrome P450
DDI: drug-drug interaction
DMSO: dimethyl sulphoxide
ESI: electrospray ionization
FDA: U.S. Food and Drug Administration
FLD: fluorescence detection
HLM: human liver microsomes
HPLC: High performance liquid chromatography
MRM: multiple-reaction monitoring mode
MS: mass spectrometry
NADP: nicotinamide adenine dinucleotide phosphate
PPL: propranolol
RdRp: RNA dependent RNA polymerase
RDV: remdesivir
SARS-CoV-2: severe acute respiratory syndrome coronavirus 2
UDPGA: uridine 5′-diphosphoglucuronic acid trisodium salt
UGT: 5'-diphospho-glucuronosyltransferase
UPLC-MS/MS: ultra-performance liquid chromatography-tandem mass spectrometry
UV: ultraviolet

Chapter 1: Introduction

1.1 Propranolol and its metabolism

Propranolol (PPL) is a non-selective competitive beta blocker which can decrease cardiac output, inhibit renin release from the kidneys, and diminish tonic sympathetic nerve outflow from vasomotor centers in the brain[1]. It is widely used as the treatment for hypertension, angina, and cardiac arrhythmia.

Propranolol is primarily metabolized by the liver and has three major metabolic pathways: ring hydroxylation, N-dealkylation followed by further side-chain oxidation, and glucuronidation[2] (Figure 1.1). These three routes account for 42%, 41% and 17% of total clearance, respectively, but contributions may vary considerably among different individuals[2]. Ring hydroxylation and N-dealkylation followed by side-chain oxidation are carried out by CYPs. With hydroxylation metabolism, the two important metabolites are 4-hydroxypropranolol and 5-hydroxypropranolol[3]. CYP2D6 is the major isozyme responsible for ring hydroxylation, whereas CYP1A2 plays a small part[3]. However, side-chain oxidation of propranolol is mainly dependent on CYP1A2 and to minor extent also mediated by CYP2D6[3]. Glucuronidation of propranolol is catalyzed by UGTs, where isozymes UGT1A9, UGT2B4 and UGT2B7 predominantly contribute to this process[4]. Via these three major metabolic routines, propranolol has four principal metabolites: 4-hydroxypropranolol, N-desisopropyl propranolol and propranolol glucuronide, and naphthyloxylactic acid[5]. Propranolol elimination is mainly dependent on the renal system and excreted as its metabolites in the urine[2].

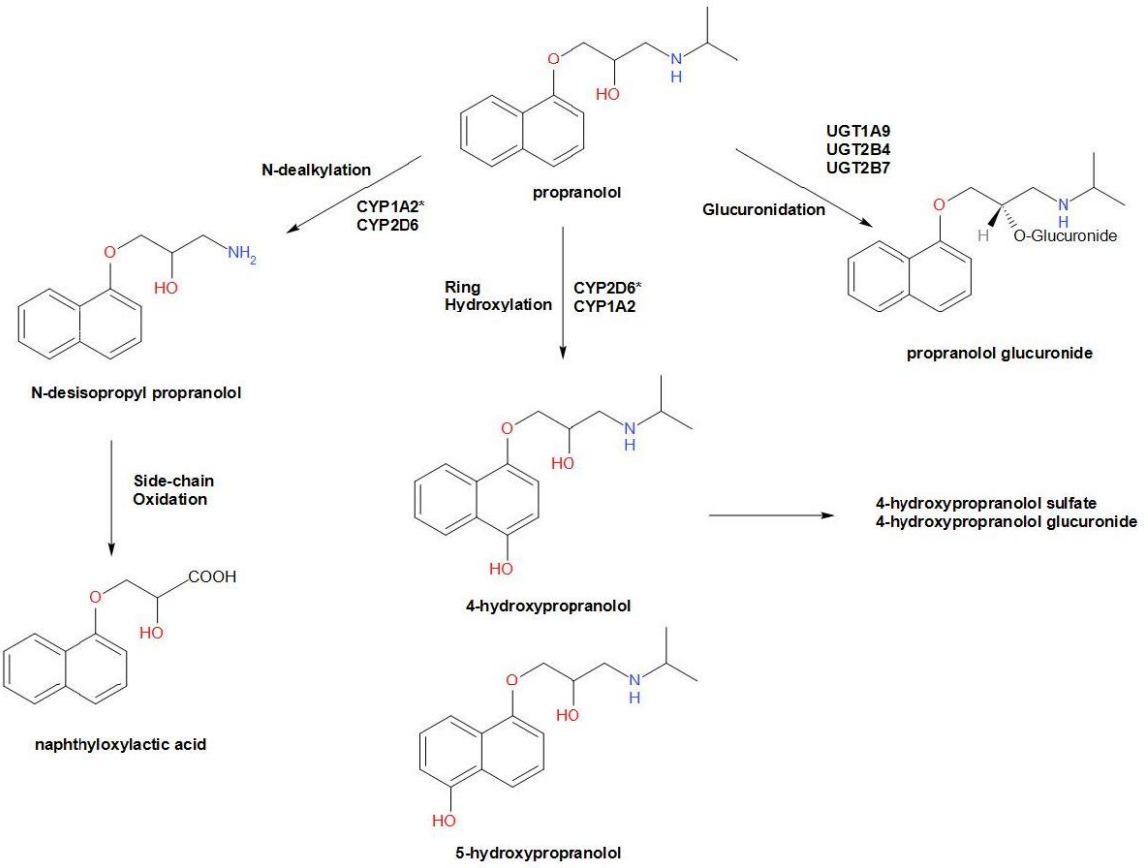

Figure 1.1. Principal metabolic pathways of propranolol. These are ring hydroxylation, N-dealkylation followed by side-chain oxidation, and glucuronidation.

1.2 Remdesivir and COVID-19

Remdesivir (GS-5734, RDV) is a stereoisomer monophosphoramidate prodrug of a nucleoside analog, which was originally developed for the treatment of Ebola virus disease and emerging viruses[6]. Severe acute respiratory syndrome coronavirus 2 (SARS-CoV-2) is a positive-sense single-stranded RNA virus, which causes coronavirus disease 2019 (COVID-19)[7,8]. COVID-19 has spread rapidly across the world, with the initial outbreak in December 2019, and has become a huge threat to global public health[9]. In Oct 2020, U.S. Food and Drug Administration (FDA) approved remdesivir (brand name: Veklury) for use in hospitalized patients as the treatment of COVID-19[10].

Remdesivir inhibits viral replication via delayed chain termination induced by its interaction with RdRp[6]. Remdesivir undergoes considerable first-pass metabolism, and is administrated by intravenous infusion instead of the oral route[11]. *In vivo*, remdesivir diffuses into cells and is first metabolized to the intermediate alanine metabolite GS-704277, which is subsequently transformed to the monophosphate nucleoside form[9]. The monophosphate nucleoside form is next converted either to the nucleoside analog GS-441524, or is rapidly phosphorylated to the active nucleoside triphosphate GS-443902[9]. GS-443902 is a substrate of viral RdRp, and competes with natural ATP substrates to induce delayed RNA chain termination during viral replication[9,12]. In addition, remdesivir and its active metabolites are highly selective for RdRps rather than human polymerases[9]. Remdesivir is a substrate for CYP2C8, CYP2D6, and CYP3A4 based on *in vitro* studies[13]. Simultaneously, remdesivir is a weak inhibitor of CYP3A4 and CYP2D6[13]. The safety profile and drug-drug interactions of remdesivir are still under development.

1.3 Potential drug-drug interactions between propranolol and remdesivir

Many COVID-19 patients have complications of hypertension and other cardiac diseases[14]. Consequently, it is of great possibility that a combination of remdesivir and propranolol might be used to treat COVID-19 patients with comorbidities. Remdesivir and propranolol are both substrates of CYP2D6 and remdesivir inhibits CYP2D6 which are the principal CYP450 enzymes involved in ring hydroxylation of propranolol. Thus, we wanted to investigate potential drug-drug interactions (DDIs) between propranolol and remdesivir.

In this study, we used an *in-vitro* incubation model based on HLM to evaluate metabolism of propranolol through CYPs and UGTs, and potential DDIs between propranolol and remdesivir. We identified metabolites of propranolol hydroxylation

carried out by CYPs using HPLC-UV and HPLC-FLD. We also monitored the propranolol glucuronide formation using HPLC-UV and determined kinetic parameters for glucuronidation. To test whether remdesivir inhibits propranolol metabolism, remdesivir was added to the reaction system, and its effect on reaction velocity for propranolol was measured using ultra-performance liquid chromatography-tandem mass spectrometry (UPLC-MS/MS). Kinetic models were applied to estimate the quantitative inhibition potency of the potential inhibitor towards propranolol metabolism. The results from this study can give us insight into *in vitro* interactions of propranolol and remdesivir, and can be used to support further DDI studies of these two drugs *in vivo*.

The figure in this chapter was drawn by myself.

Chapter 2: Methods and Materials

2.1 Chemicals and reagents

Propranolol was obtained from Key Organics (Bedford, MA, USA). 4-hydroxypropranolol and 5-hydroxypropranolol were purchased from Cayman Chemical (Ann Arbor, MI, USA). 4-hydroxypropranolol (1 mg/mL) and 5-hydroxypropranolol (1 mg/mL) stock solutions were prepared in dimethyl sulphoxide (DMSO). Propranolol (50 uM) and remdesivir (4.15 mM) stock solutions were prepared by dissolving in methanol. These stock solutions were all kept at -20℃ and further diluted with methanol for experimental use. DL-isocitric acid, β-nicotinamide adenine dinucleotide phosphate sodium salt hydrate (NADP), uridine 5′-diphosphoglucuronic acid trisodium salt (UDPGA), isocitric dehydrogenase, and alamethicin were obtained from Sigma-Aldrich (St. Louis, MO, USA). HPLC and MS grade ultrapure water and organic solvents were purchased from Thermo Fisher Scientific (Waltham, MA, USA).

2.2 Laboratory methods

2.2.1 *In-vitro* microsomal incubation system

An *in-vitro* microsomal incubation system was performed following previously published methods[15]. The system contains human liver microsomes, propranolol with and without remdesivir, and other cofactors essential for the reaction.

2.2.2 Preparation of human liver microsomes

The method for preparation of HLM was described previously[16]. Briefly, human liver tissue was thawed at 4 °C and homogenized three times (w/v) in homogenization buffer (250 mM sucrose and 66.7 mM KH_2PO_4-Na_2HPO_4 at pH = 7.4), then differentially

centrifuged at 900 g for 10 minutes, 13500 g for 10 minutes, and 105000 g for 30 minutes. The final sediment was collected and suspended in homogenizing buffer and centrifuged at 105000 g again, and resuspended in 50 mM KH_2PO_4 buffer (pH = 7.4). The microsomes were stored at -80 °C until use. The protein concentration in the HLMs was determined by the bicinchoninic acid assay.

HLM#	830	866	Pooled
Donor's gender	Male	Male	Mixed
Donor's age	43	21	Mixed
Concentration of stock solution (mg/mL)	33.7	23.8	16.8

Table 2.1 Human liver microsome information

2.2.3 CYP reaction system

CYP reaction system was designed based on the previous reports[17]. A total 250 uL incubation mixture contains 0.1 mg/mL HLM, 50 mM KH_2PO_4 buffer (pH=7.5), cofactors, and a series of concentrations of propranolol with or without inhibitor dependent on the specific experiment. Different volumes of stock propranolol were added to the centrifuge tubes, and the solvent was evaporated at room temperature. The HLM concentration was chosen based on preliminary studies, with the objective of generating a detectable amount of metabolite with the lowest HLM concentration to avoid the interference by non-specific binding. The cofactor mixture contained 5 mM $MgCl_2$, 0.5 mM NADP, 3.75 mM DL-isocitric acid, and 1 unit/mL of isocitric dehydrogenase as a NADPH+ regeneration system[18]. All concentrations were based on a 250 uL incubation mixture.

2.2.4 UGT reaction system

The UGT reaction system was designed based on review of previous literature[19]. The total 250 uL incubation mixture contained 0.25 mg/mL of microsomes, 5 mM uridine UDPGA to provide glucuronide acid, and 5 mM $MgCl_2$. 50 mM KH_2PO_4 solution was used to maintain a physiological pH of 7.35-7.40[17]. Before initiation, alamethicin was added to the microsomes, and the mixture was kept on ice for 20 mins to fully activate the UGTs[20,21].

2.2.5 Incubation procedure

A series of concentrations of propranolol with and without remdesivir in tubes were put into an evaporator to remove the solvent. The cofactor mixture was premade to an intermediate concentration, kept on ice, and added to the system to start the reaction. After initiation, the incubation tubes were kept at 37 °C in a water bath with gentle shaking for 30 mins for CYP, and 1 hour for UGT, based on the preliminary findings. 100 uL of acetonitrile was added to the system to stop the reaction. Samples were then centrifuged at 14000 rpm for 10 minutes to separate the protein, and the supernatant was collected and used for the assay.

2.3 Metabolite identification

2.3.1 HPLC-UV

The main metabolites of propranolol hydroxylation were 4-hydroxypropranolol and 5-hydroxypropranolol (see introduction part). 150 uM standards of PPL, 4-OH PPL, and 5-OH PPL were injected into the HPLC system using an Agilent (Santa Clara, CA,

USA) Poroshell 120 EC-C18 column. The UV detector was set to a full wavelength scan mode. I optimized the methods by altering the elution parameters. The mobile phase gradient went from 50 % ACN: 50 % 10 mM NH_4COOH buffer (pH = 3) to 20 % ACN: 80 % NH_4COOH buffer (pH = 3), changed by 10% each time. We repeated the alteration of mobile phase gradient under pH = 6 situation. The best conditions appeared to be 25 % ACN with 75 % NH_4COOH buffer (pH = 3), which were chosen by the criteria that have a good peak shape while maintaining the retention time of PPL to be no more than 10 minutes.

2.3.2 HPLC-FLD

The HPLC conditions for HPLC-FLD were the same as HPLC-UV. The excitation and emission wavelengths of PPL and 4-OH PPL were set to 285/345 nm and 285/420 nm, respectively[22,23]. FLD was also set emission full wavelength scan mode with excitation at 285 nm due to lack of literature for the 5-OH PPL FLD detection properties. The final FLD detection wavelength for 5-OH PPL was set to 285/335 nm based on the scan result.

2.3.3 UPLC-MS/MS

A 10-minute gradient method was used for the UPLC system. The initial 95 % H_2O with 5 % ACN was held for 1.5 minutes, decreased to 10 % in 3.5 minutes, and kept for 2 minutes, rapidly increased back to 95 % in 0.2 minutes, and kept to the end. A Water Acquity (Milford, MA, USA) UPLC CSH C18 17 um 2.1*100 mm column was used for analysis. The ion source of MS was switched to electrospray ionization (ESI), in the multiple-reaction monitoring mode (MRM). For PPL and OH-PPL, MS conditions were tuned using standards. Based on the results, Q1/Q3 mass were 260.103/183.008, 276.103/199.008 da/z, collision potentials were set to 25 and 47 volts. collision cell exit

potentials were set to 4 and 50 volts. Other minor Q3 fragments were also included in the method.

2.4 Kinetic models

2.4.1 Reaction model

The enzyme amount in the reaction procedure did not change. The kinetic model we used was the Michaelis-Menten model (Equation 1)[24]:

$$V = \frac{Vmax[S]}{Km + [S]} \quad [Eq. 1]$$

Iterated variables were: Km: substrate concentration at half of maximum reaction velocity, Vmax: maximum reaction velocity. Data points were: [S]: substrate concentration, V: reaction velocity.

2.4.2 IC50

To determine the IC50 of the inhibitor, we used the Hill equation (Equation 2) to model the inhibition effect.

$$Inhibition = \frac{Emax[I]^r}{[I]^r + IC^r} \quad [Eq. 2]$$

The original equation was modified to the form below (Equation 3) to fit our study as previously established. The substrate concentration was fixed and chosen to be close to the Km from the Michaelis-Menten relationship.

$$Rv = 100\left(1 - \frac{Emax[I]^r}{[I]^r + IC^r}\right) \quad [Eq. 3]$$

Iterated variables were: r: exponent in Hill equation, IC: inhibitor concentration producing 50% of maximum effect, Emax: maximum effect. Data points were: [I]: inhibition concentration. Rv: reaction velocity expressed as percentage of control velocity without inhibitor. Then, the actual IC50 was calculated using Equation 4:

$$IC50 = \frac{IC}{(2Emax - 1)^{1/r}} \quad [Eq. 4]$$

IC50: inhibitor concentration at reducing reaction velocity to 50% of control velocity.

The human liver microsomes were kindly prepared by Ms. Suxiang Duan. The development of HPLC-UV, HPLC-FLD and UPLC-MS/MS methods for metabolite identification was done by Mr. Qingchen Zhang and me.

Chapter 3: Results

3.1 *In-vitro* metabolism of propranolol via CYP450

3.1.1 HPLC-UV detection of propranolol and its metabolites

Initially, the UV detector was set to a full wavelength scan mode to detect propranolol, 4-hydroxypropranolol, and 5-hydroxypropranolol at one acquisition, which may have different absorbance maxima. The mobile phase was composed of ACN and NH_4COOH buffer. We changed the ACN percentage from 20 % to 80 % at pH = 3 or pH = 6. The retention times of propranolol, 4-hydroxypropranolol, and 5-hydroxypropranolol are provided below (Table 3.1). In order to obtain better peak shapes, and keep the retention time of propranolol within 10 minutes (Figure 3.1-3.2), the final HPLC-UV detection method was: (1) mobile phase: ACN: NH_4COOH (v/v: 25:75, pH = 3), (2) UV wavelength: 222 nm, (3) injection volume: 10 uL, (4) flow rate: 1 mL/min

NH_4COOH Percentage	Retention Time (min) pH = 3			Retention Time (min) pH = 6		
	PPL	4-OH PPL	5-OH PPL	PPL	4-OH PPL	5-OH
50%	0.772	0.656	0.651	0.816	0.667	0.660
60%	1.017	0.742	0.721	1.904	0.753	0.730
70%	2.018	0.977	0.900	2.207	1.025	0.929
80%	8.478	2.246	1.680	9.561	2.443	1.803

Table 3.1. Retention times of propranolol, 4-hydroxypropranolol, and 5-hydroxypropranolol with different mobile phases and pH conditions.

We then used this method to analyze combined standards of 150 uM propranolol, 4-hydroxypropranolol, and 5-hydroxypropranolol. The retention times of these three compounds are 4.54 min, 1.50 min, and 1.23 min, respectively (Figure 3.2).

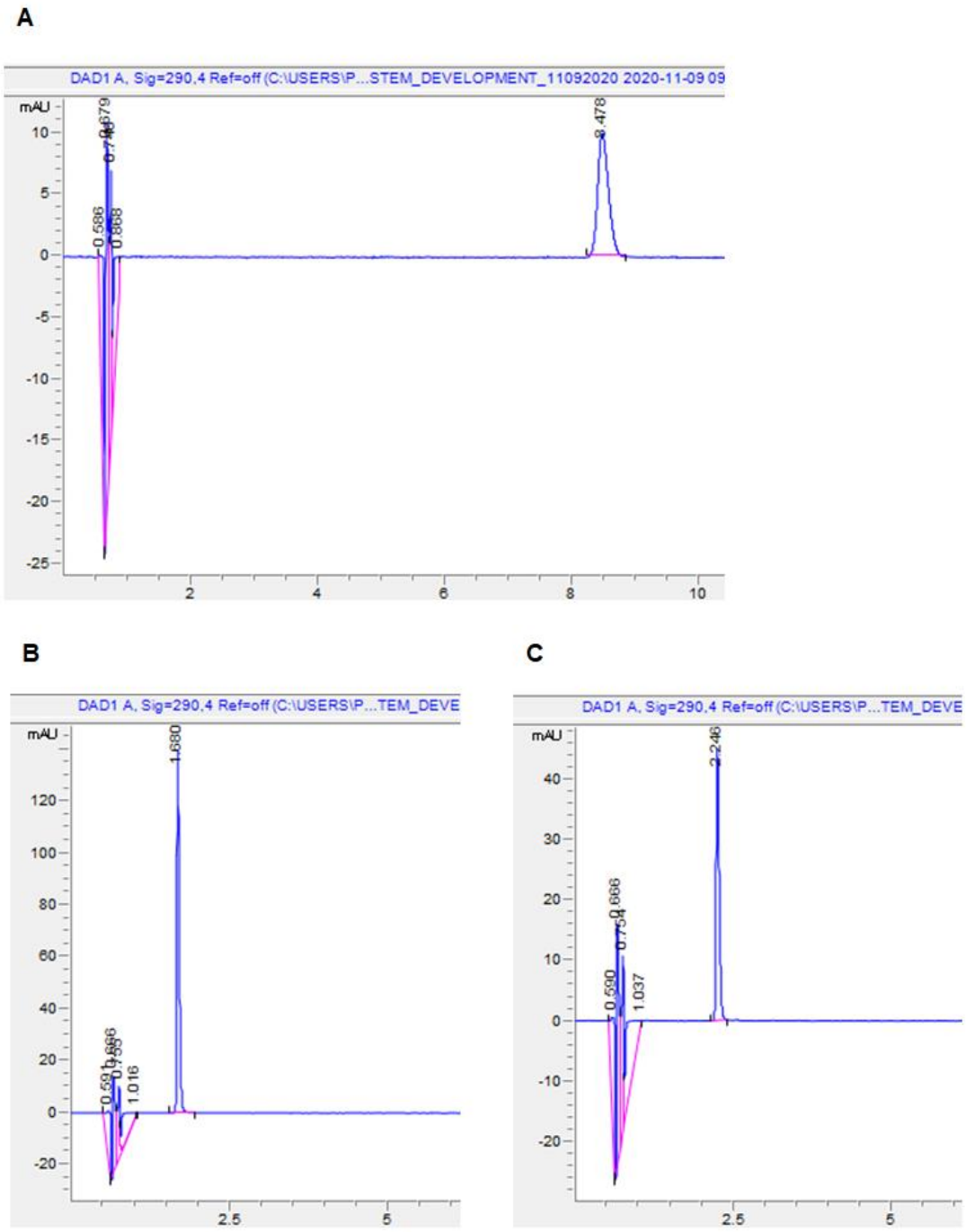

Figure 3.1. Chromatographic peaks for propranolol, 4-hydroxypropranolol and 5-hydroxypropranolol during HPLC-UV method development. The conditions were 20% ACN at pH = 3. A: propranolol, retention time: 8.50 min, B: 4-hydroxypropranolol, retention time: 2.25 min, C: 5-hydroxypropranolol, retention time: 1.68 min.

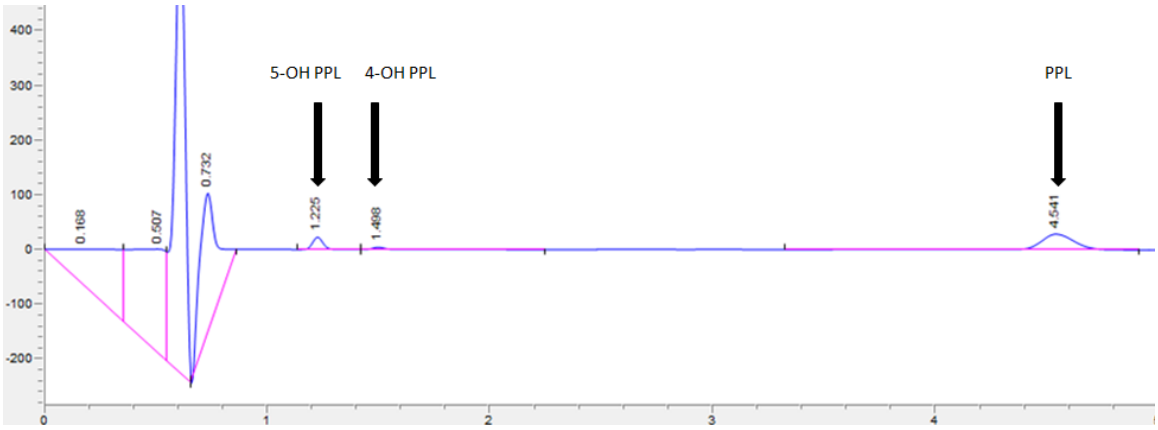

Figure 3.2. Identification of propranolol, 4-hydroxypropranolol, and 5-hydroxypropranolol through HPLC-UV detection

3.1.2 HPLC-FLD of propranolol and its metabolites

In order to confirm and improve the identification of propranolol and its metabolites, we used HPLC-fluorescence detection as well. HPLC-fluorescence assays of propranolol and 4-hydroxypropranolol has been reported several times, but 5-hydroxypropranolol analysis is rarely investigated[22,23]. Thus, we developed the HPLC-fluorescence detection method for 5-hydroxypropranolol. Initially, we selected 285 nm as the excitation wavelength based on its UV absorption, then we scanned emission wavelength from 200 nm to 400 nm to identify the best emission wavelength. We found 344 nm is the ideal emission wavelength for 5-hydroxypropranolol (Figure 3.3).

We also used the fluorescence method to identify propranolol and 4-hydroxpropranolol. When the excitation wavelength was 285 nm and emission wavelength was 420 nm, we can detect propranolol and its two hydroxy metabolites simultaneously (Figure 3.4). The retention times for 4-hydroxypropranolol, 5-hydroxypropranolol, and propranolol were 1.51 min, 1.24 min and 4.64 min, respectively (Figure 3.4).

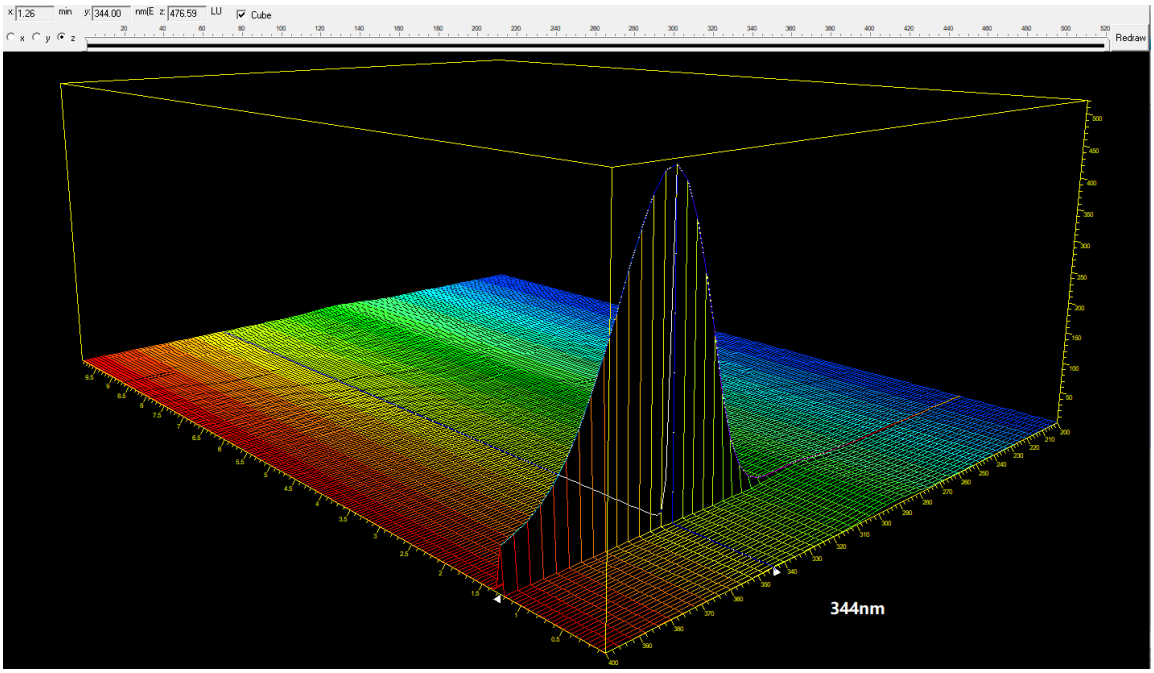

Figure 3.3. 3D plot of 5-hydroxypropranolol emission wavelength scan. The X-axis is retention time, The Y-axis is emission wavelength, and The Z-axis is intensity.

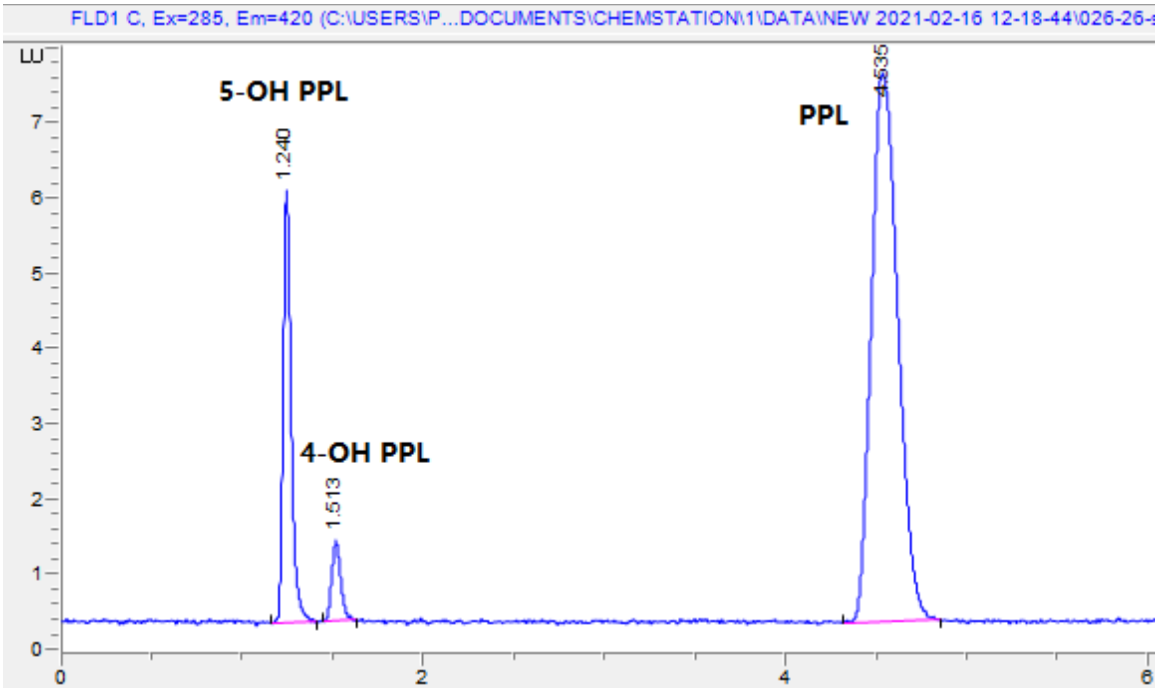

Figure 3.4. HPLC-fluorescence analysis of 4-hydroxypropranolol, 5-hydroxypropranolol, and propranolol. X-axis is retention time (min). LU=luminescence units.

3.1.3 UPLC-MS/MS detection of propranolol and its metabolites

Although we can identify propranolol, 4-hydroxypropranolol, and 5-hydroxypropranolol using HPLC-UV or HPLC-FLD, after incubation of propranolol and HLMs, metabolites generation was insufficient for reliable quantitation, even at 250 uM propranolol. Consequently, we used UPLC-MS to detect propranolol and its hydroxylation metabolites, which is more sensitive and can detect lower concentrations. The results are shown in Figure 3.5.

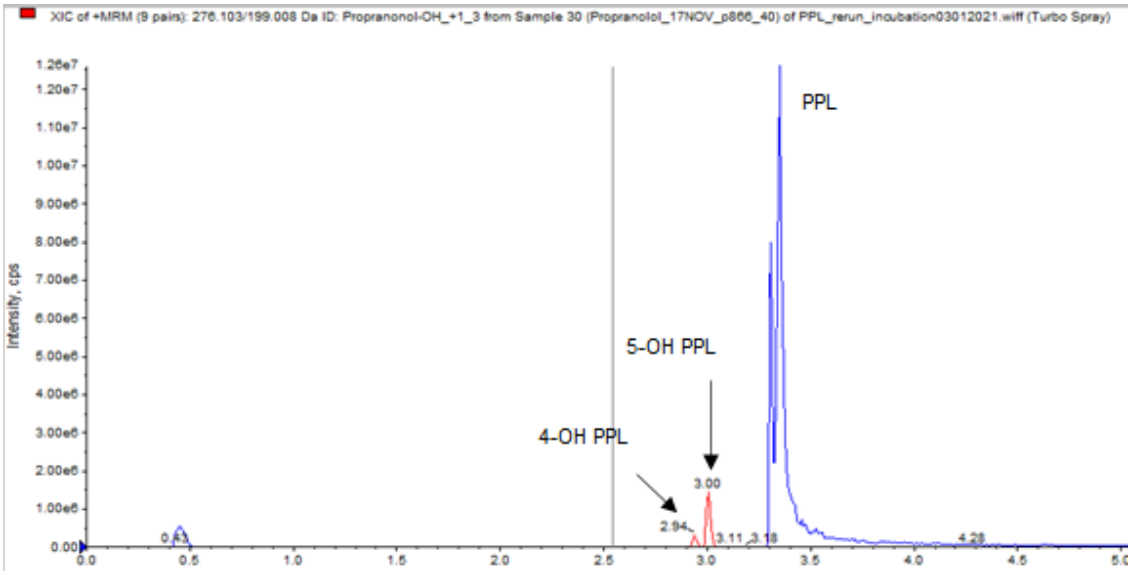

Figure 3.5. Mass spectrometric peaks for the mixture of propranolol, 4-hydroxypropranolol and 5-hydroxypropranolol standards. The retention times were 3.35 min, 2.94 min and 3.00 min, respectively.

3.1.4 The kinetics of propranolol hydroxylation

We first confirmed the linearity between MS response and compound concentration (Figure 3.6). The MS response of 4-hydroxypropranolol and 5-hydroxypropranolol were linearly related to concentrations. Thus, MS response was used as a surrogate to reflect reaction velocity.

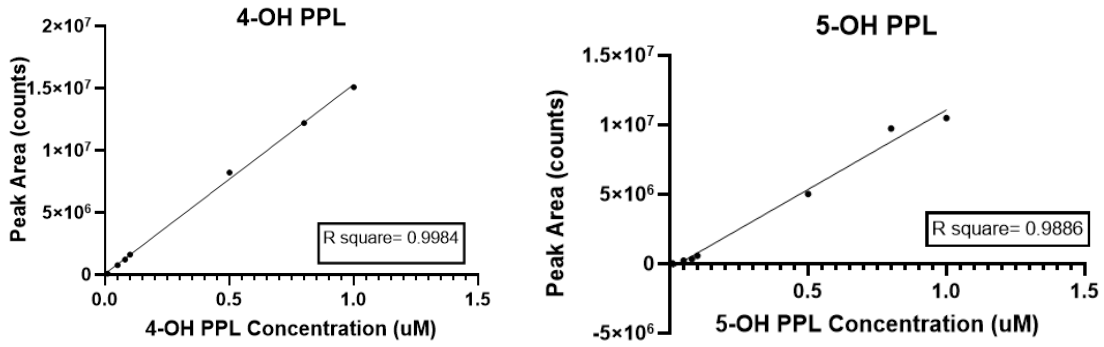

Figure 3.6. The relation of peak area and concentrations of metabolites

To research the kinetics of propranolol hydroxylation, we fixed the incubation time at 30 mins, and added different concentrations of propranolol (0, 0.25, 0.75, 1.25, 2.5, 5, 10, 20, 40, 80, 100, 150, 175, 250 uM) to reaction systems with three different HLMs (830, 866, pooled). The Michaelis-Menten model equation [Eq. 1] was fitted to data points (metabolite formation rate versus substrate concentration) and the Km and Vmax were determined by non-linear regression (Figure 3.7- 3.9). The Km for pooled HLM reaction system was 19.9 uM for 4-hydroxypropranolol, and 17.9 uM for 5-hydroxypropranolol (Figure 3.7).

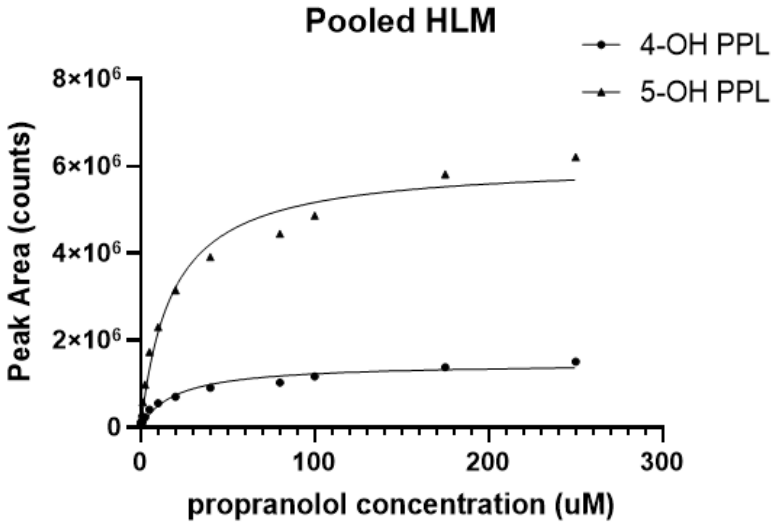

Figure 3.7. Propranolol incubation with pooled HLM. 4-OH PPL: Km = 19.8 uM, R square=0.97. 5-OH PPL: Km = 18.0 uM, R square = 0.98

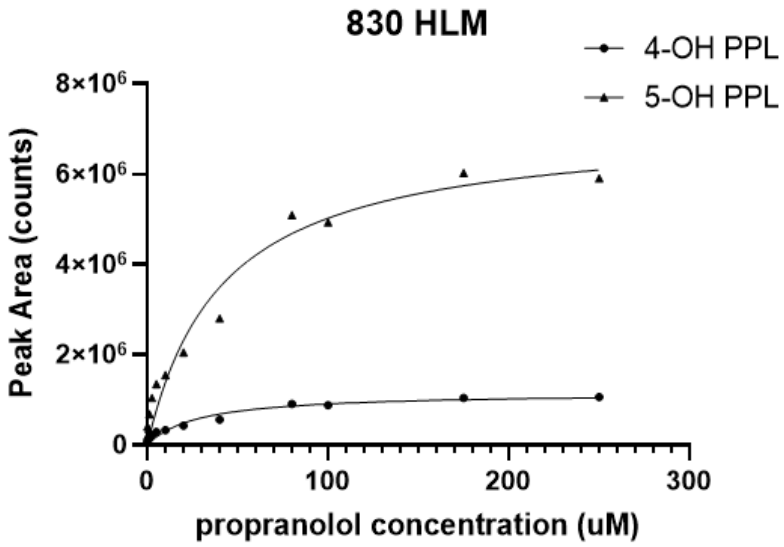

Figure 3.8. Propranolol incubation with 830 HLM. 4-OH PPL: Km = 27.9 uM, R square = 0.96. 5-OH PPL: Km = 41.4 uM, R square = 0.96

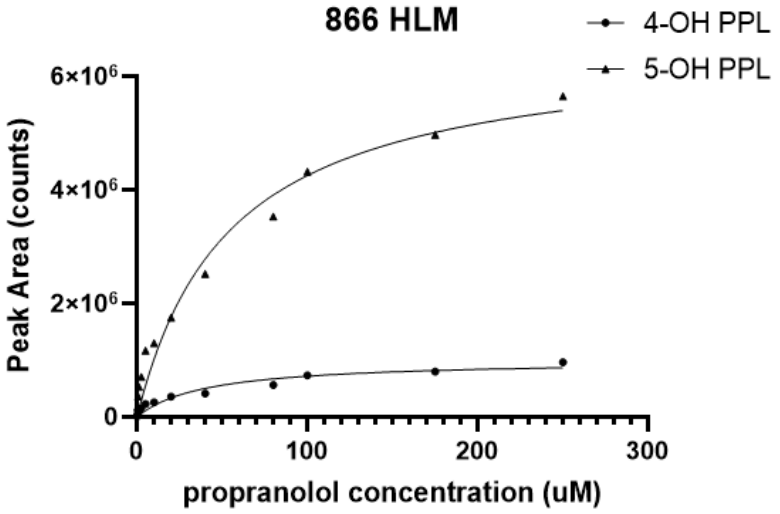

Figure 3.9. Propranolol incubation with 866 HLM. 4-OH PPL: Km = 39.5 uM, R square = 0.94. 5-OH PPL: Km = 54.6 uM, R square = 0.97

3.2 *In vitro* study of propranolol glucuronidation via UGTs

As in the study of propranolol metabolism via CYP450, we next investigated the kinetics of propranolol glucuronidation via UGTs. With the *in-vitro* UGT metabolic

conditions (method 2.1.4), propranolol glucuronide was detected, and the peak height was recorded using HPLC-UV. The Michaelis-Menten model equation [Eq. 1] was used to analyze data. Km was 284 uM (Figure 3.10).

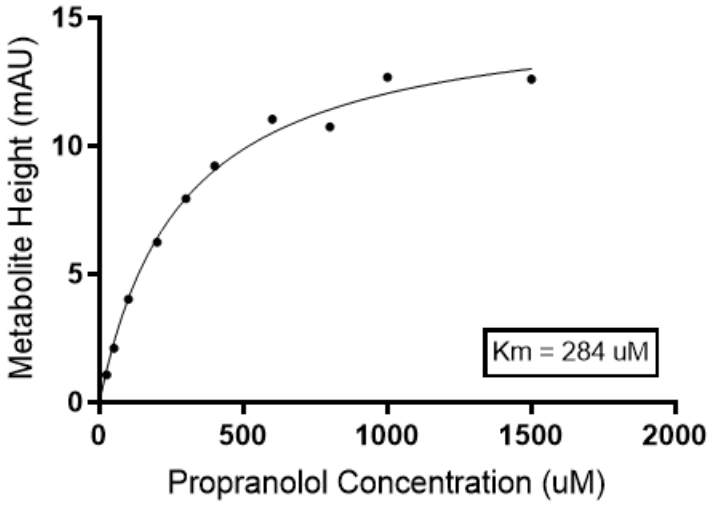

Figure 3.10. Propranolol glucuronide formation of the incubation with pooled HLM. Km = 284 uM, R square = 0.99.

3.3 *In vitro* inhibition of propranolol metabolism by remdesivir

Because remdesivir and propranolol are both substrates of CYP2D6, we mainly estimated the inhibitory effect of remdesivir on ring hydroxylation of propranolol. To estimate the IC50 of remdesivir, we picked a concentration close to the Km of propranolol (15 uM). After adding different concentrations of remdesivir (0, 1.25, 2.5, 5, 10, 25, 50 uM), we measured the metabolite formation rates of 4-hydroxypropranolol and 5-hydroxypropranolol. Then, equation 3 was fitted to the data points and we obtained the results shown in Fig. 3.10. When the concentration of propranolol was 15 uM, the Emax of remdesivir was 0.45, r = 0.73 and IC was 0.59 uM for 4-hydroxypropranolol and the Emax = 0.67, r = 0.45 and IC = 25.4 uM for 5-hydroxypropranolol. Because the maximal effect of remdesivir in inhibiting propranolol 4-hydroxylation did not exceed 0.5, we could

not obtain an IC50 for inhibition of 4-hydroxypropranolol formation by remdesivir. We then calculated the IC50 for inhibition of 5-hydroxypropranolol (at 15 uM propranolol) using [Eq.4], and obtained the result the IC50 value was 279 uM.

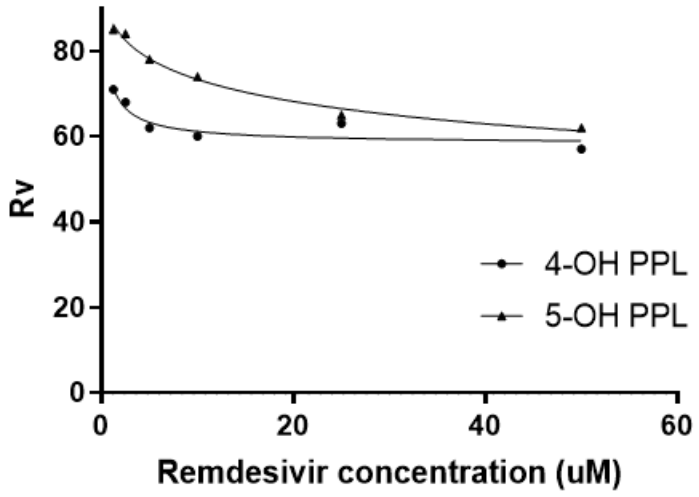

Figure 3. 11. Inhibition by remdesivir at 15 uM propranolol. Inhibition for 4-OH PPL formation: Emax = 0.42, r = 0.86 IC = 0.51 uM, and R square = 0.85. Inhibition for 5-OH PPL formation: Emax = 0.67, r = 0.45, IC = 25.4 uM and R square = 0.98. IC50 = 279 uM.

All figures in this part were done by myself. Mr. Qingchen Zhang kindly helped me with HPLC-UV method development and 5-hydroxypropranolol emission wavelength scan work. Other works were finished by myself.

Chapter 4: Discussion

In this *in vitro* model study, we first identified propranolol, 4-hydroxypropranolol and 5-hydroxypropranolol using the HPLC-UV method. In previous studies, 5-hydroxypropranolol was not commonly evaluated in propranolol metabolism studies, whereas propranolol and 4-hydroxypropranolol were identified and quantitated in most cases[22,23]. Thus, we developed a HPLC-UV detection method to assay propranolol and its two metabolites simultaneously. We also established a HPLC-FLD method to detect 5-hydroxypropranolol using emission wavelength scans, demonstrating an optimal excitation wavelength of 285 nm, and the best emission wavelength at 344 nm. To confirm and measure propranolol and its metabolites with greater sensitivity, we next used HPLC-FLD to identify the three compounds. However, it was not possible to reliably quantitate the metabolites from incubation samples because of low quantitative generation. Therefore, we used UPLC-MS/MS to determine the levels of the metabolites. Based on the data from UPLC-MS/MS, the Michaelis-Menten model was applied to calculate the kinetic parameters for propranolol hydroxylation through CYP450 metabolic pathways, and we obtained Km values of 19.8 uM and 18.0 uM for 4-hydroxypropranolol and 5-hydroxyprorpanolol in pooled HLM.

We also measured propranolol glucuronide produced by UGTs *in vitro* using HPLC-UV, and obtained kinetic results for propranolol glucuronidation, which has not been extensively investigated in previous studies. Using the Michaelis-Menten model, the Km value was found to be 284 uM.

Because CYP pathways accounts for the majority (83%) of the total metabolism, and propranolol and remdesivir are both substrates of CYP2D6, we next investigated the inhibition of propranolol hydroxylation by remdesivir[2]. When the concentration of

propranolol was 15 uM, the maximum extent of inhibition by remdesivir (Emax) was 0.45, and the IC was 0.59 uM for 4-hydroxypropranolol formation. Because the maximal inhibition of 4-hydroxypropranolol formation did not exceed 0.50, we could not determine an IC50 value. The IC50 for inhibition of 5-hydroxypropranolol formation was 279 uM. These results indicate that showed us remdesivir produces only weak inhibition effect of propranolol metabolism. It confirmed the conclusion that remdesivir weakly inhibits CYP2D6 in previous reports[13]. In clinical practice, remdesivir is administered intravenously using a 200 mg loading dose, followed by 100 mg administered daily (day 2 to day 10) as a maintenance dose[25]. The Cmax values in healthy humans were approximately 4380 ng/ml (7.26 uM) on day 1, and 2230 ng/ml (3.70 uM) on day 5 in a Phase I study[26]. Thus, clinically important inhibition of propranolol metabolism. Though remdesivir is not a strong inhibitor of propranolol biotransformation, the results still remind us to pay attention to the combination drug therapy with these two drugs during clinical use.

Clinical drug-drug interactions of remdesivir still remain unclear. Based on the CYP metabolism of remdesivir, a previous study discussed the potential DDIs between remdesivir and some pulmonary drugs, such as rifabutin and metamizole[27]. The FDA has warned that remdesivir should not be administered with chloroquine phosphate or hydroxychloroquine sulfate due to the antagonistic effect of chloroquine on the antiviral activity of remdesivir based on nonclinical data. However, due to its short half-life (around 1 hour), remdesivir is transformed and degraded rapidly *in vivo*[28]. Remdesivir is believed to have limited clinically significant DDIs[28]. Remdesivir is mainly (80%) transformed to GS-704277 by hydrolytic cleavage via carboxylesterase 1 (CES1)[29]. Rifampin, a potent inducer of CES1 and CYP3A4, is expected to reduce remdesivir

exposure by 30%[29]. More clinical study and in vivo data are needed to investigate DDIs involving remdesivir.

Future directions of this study would involve the effects of the intermediate alanine metabolite GS-704277 (half-life: 1.7 hours), and the nucleoside analog GS-441524 (half-life: 25 hours) on propranolol metabolism[30]. In addition, the enzymes responsible for GS-704277 and GS-441524 metabolism have not described. This would provide additional scientific information in the pharmacokinetics of remdesivir, and potential interactions with other drugs. Remdesivir is still a relatively new drug, and data of this type will be of help forward the objective of safe and effective treatment with remdesivir.

`

Chapter 5: Bibliography

1. Weber MA, Drayer JI. Renal effects of beta-adrenoceptor blockade. *Kidney Int.* 1980;18(5):686-699.
2. Walle T, Walle UK, Olanoff LS. Quantitative account of propranolol metabolism in urine of normal man. *Drug Metab Dispos.* 1985;13(2):204-209.
3. Upthagrove AL, Nelson WL. Importance of amine pKa and distribution coefficient in the metabolism of fluorinated propranolol analogs: metabolism by CYP1A2. *Drug Metab Dispos.* 2001;29(11):1389-1395.
4. Hanioka N, Hayashi K, Shimizudani T, et al. Stereoselective glucuronidation of propranolol in human and cynomolgus monkey liver microsomes: role of human hepatic UDP-glucuronosyltransferase isoforms, UGT1A9, UGT2B4 and UGT2B7. *Pharmacology.* 2008;82(4):293-303.
5. Silberx BM, Holford NHG, Riegelman S. Dose-Dependent Elimination of Propranolol and its Major Metabolites in Humans. *Journal of Pharmaceutical Sciences.* 1983;72(7):725-732.
6. Siegel D, Hui HC, Doerffler E, et al. Discovery and Synthesis of a Phosphoramidate Prodrug of a Pyrrolo[2,1-f][triazin-4-amino] Adenine C-Nucleoside (GS-5734) for the Treatment of Ebola and Emerging Viruses. *J Med Chem.* 2017;60(5):1648-1661.
7. Goldman JD, Lye DCB, Hui DS, et al. Remdesivir for 5 or 10 Days in Patients with Severe Covid-19. *N Engl J Med.* 2020;383(19):1827-1837.
8. Machhi J, Herskovitz J, Senan AM, et al. The Natural History, Pathobiology, and Clinical Manifestations of SARS-CoV-2 Infections. *J Neuroimmune Pharmacol.* 2020;15(3):359-386.
9. Eastman RT, Roth JS, Brimacombe KR, et al. Remdesivir: A Review of Its Discovery and Development Leading to Emergency Use Authorization for Treatment of COVID-19. *ACS Cent Sci.* 2020;6(5):672-683.
10. Bravo JPK, Dangerfield TL, Taylor DW, Johnson KA. Remdesivir is a delayed translocation inhibitor of SARS-CoV-2 replication. *Mol Cell.* 2021.
11. Cao YC, Deng QX, Dai SX. Remdesivir for severe acute respiratory syndrome coronavirus 2 causing COVID-19: An evaluation of the evidence. *Travel Med Infect Dis.* 2020;35:101647.
12. Jorgensen SCJ, Kebriaei R, Dresser LD. Remdesivir: Review of Pharmacology, Pre-clinical Data, and Emerging Clinical Experience for COVID-19. *Pharmacotherapy.* 2020;40(7):659-671.
13. Yang K. What Do We Know About Remdesivir Drug Interactions? *Clinical and Translational Science.* 2020;13(5):842-844.
14. Weiss P, Murdoch DR. Clinical course and mortality risk of severe COVID-19. *Lancet.* 2020;395(10229):1014-1015.
15. Greenblatt DJ, Zhao Y, Venkatakrishnan K, et al. Mechanism of cytochrome P450-3A inhibition by ketoconazole. *J Pharm Pharmacol.* 2011;63(2):214-221.
16. Chamberlain J, Jagarinec N, Ofner P. Catabolism of C19-steroids by subcellular fractions of mammalian and avian tissues. I. Hydroxylation of ring A-saturated substrates by rat-liver microsomes. *Steroids.* 1965:Suppl 2:1-12.
17. Volak LP, Greenblatt DJ, von Moltke LL. In Vitro Approaches to Anticipating Clinical Drug Interactions. In: *Drug–Drug Interactions in Pharmaceutical Development.*2007:31-74.
18. von Moltke LL, Greenblatt DJ, Harmatz JS, Shader RI. Alprazolam metabolism in vitro: studies of human, monkey, mouse, and rat liver microsomes. *Pharmacology.* 1993;47(4):268-276.

19. Court MH. Isoform-selective probe substrates for in vitro studies of human UDP-glucuronosyltransferases. *Methods Enzymol.* 2005;400:104-116.
20. Ladd MA, Fitzsimmons PN, Nichols JW. Optimization of a UDP-glucuronosyltransferase assay for trout liver S9 fractions: activity enhancement by alamethicin, a pore-forming peptide. *Xenobiotica.* 2016;46(12):1066-1075.
21. Walsky RL, Bauman JN, Bourcier K, et al. Optimized assays for human UDP-glucuronosyltransferase (UGT) activities: altered alamethicin concentration and utility to screen for UGT inhibitors. *Drug Metab Dispos.* 2012;40(5):1051-1065.
22. Albani F, Riva R, Baruzzi A. Simple and rapid determination of propranolol and its active metabolite, 4-hydroxypropranolol, in human plasma by liquid chromatography with fluorescence detection. *J Chromatogr.* 1982;228:362-365.
23. Miller RB. High-performance liquid chromatographic assay for the derivatized enantiomers of propranolol and 4-hydroxypropranolol in human plasma. *J Pharm Biomed Anal.* 1991;9(10-12):953-958.
24. Michaelis L, Menten ML, Johnson KA, Goody RS. The original Michaelis constant: translation of the 1913 Michaelis-Menten paper. *Biochemistry.* 2011;50(39):8264-8269.
25. Durante-Mangoni E, Andini R, Bertolino L, et al. Early experience with remdesivir in SARS-CoV-2 pneumonia. *Infection.* 2020;48(5):779-782.
26. Humeniuk R, Mathias A, Kirby BJ, et al. Pharmacokinetic, Pharmacodynamic, and Drug-Interaction Profile of Remdesivir, a SARS-CoV-2 Replication Inhibitor. *Clinical Pharmacokinetics.* 2021.
27. Gandhi Z, Mansuri Z, Bansod S. Potential Interactions of Remdesivir with Pulmonary Drugs: a Covid-19 Perspective. *SN Compr Clin Med.* 2020:1-2.
28. Rezaee H, Pourkarim F, Pourtaghi-Anvarian S, Entezari-Maleki T, Asvadi-Kermani T, Nouri-Vaskeh M. Drug-drug interactions with candidate medications used for COVID-19 treatment: An overview. *Pharmacol Res Perspect.* 2021;9(1):e00705.
29. Humeniuk R, Mathias A, Kirby BJ, et al. Pharmacokinetic, Pharmacodynamic, and Drug-Interaction Profile of Remdesivir, a SARS-CoV-2 Replication Inhibitor. *Clin Pharmacokinet.* 2021.
30. Tempestilli M, Caputi P, Avataneo V, et al. Pharmacokinetics of remdesivir and GS-441524 in two critically ill patients who recovered from COVID-19. *J Antimicrob Chemother.* 2020;75(10):2977-2980.